Accurate Reconstruction of the Standard 12-Lead ECG from a Single Lead based on Inherent Principles of ECG

Dong-hyuk Seo[1], Ui Jong Kim[1], Yong-Yeon Jo[2], Junmyung Kwon[2], Won-Yong Shin[3], and Sang-Wook Kim[1⋆]

[1] Hanyang University, Korea
hyuk125@hanyang.ac.kr, kimgb6060@hanyang.ac.kr, wook@hanyang.ac.kr
[2] Medical AI Inc., Korea
yy.jo@medicalai.com, jm.kwon@medicalai.com
[3] Yonsei University, Korea
wy.shin@yonsei.ac.kr

Abstract. Wearable and portable devices enable convenient electrocardiography (ECG) acquisition, yet they typically measure only a single limb lead, limiting diagnostic utility compared to the standard 12-lead ECG used in hospitals. We study the problem of generating the full standard 12-lead ECG from a single measured lead by leveraging inherent ECG principles. Specifically, we emphasize two claims: (i) limb lead reconstruction benefits from a hybrid strategy that generates only one additional limb lead via learning and computes the remaining limb leads through vector operations; and (ii) precordial lead reconstruction is more reliable when conditioned on the full set of limb leads. Based on these claims, we propose **AURORA**, a 12-lead ECG reconstruction framework that combines learning models and deterministic vector operations to generate limb leads, followed by the reconstruction of precordial leads. To instantiate the learning components, we propose **IGUANA**, a lead-pattern learning model comprising a lead representation learner and a lead generator for precise lead-to-lead transformation. Experiments on two benchmark datasets demonstrate that AURORA consistently outperforms state-of-the-art methods and validate the effectiveness of incorporating vector operations in lead reconstruction. Our code is available at `https://github.com/DHSeo11/AURORA.git`.

Keywords: ECG reconstruction · Vector operation of ECG · Generative deep learning.

1 Introduction

Electrocardiography (ECG) is a widely used, non-invasive tool for diagnosing cardiovascular diseases that are often difficult to identify based on symptoms alone [11,19]. In clinical environments, standard ECG acquisition records the

⋆ Corresponding author.

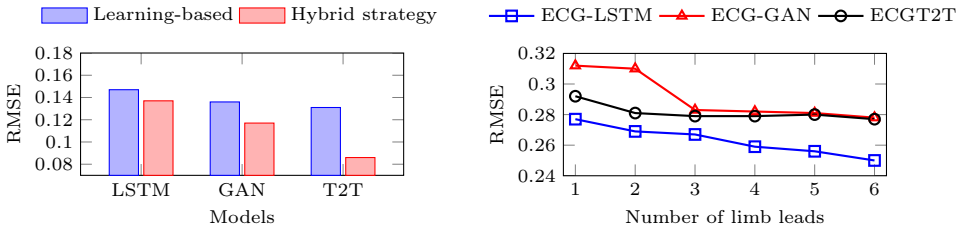

Fig. 1. RMSE comparison. (Left) Comparing Reconstruction types across models. (Right) Varying the number of limb leads.

standard 12-lead ECG, consisting of six limb leads (I, II, III, aVR, aVL, aVF) and six precordial leads (V1–V6), thereby providing comprehensive cardiac views. Despite its clinical utility, this standard setup requires hospital infrastructure and is thus unsuitable for continuous, out-of-hospital monitoring.

To overcome this limitation, portable or wearable ECG devices have rapidly emerged for ubiquitous monitoring [2,3,1]. However, due to hardware and form-factor constraints, such devices typically measure only a *single* limb lead (e.g., Lead I) [2,22,17], which inherently restricts diagnostic potential compared to the standard 12-lead ECG. This motivates an important yet challenging problem: *accurate reconstruction of the standard 12-lead ECG from a single measured lead.* While recent deep-learning methods have explored end-to-end lead translation [14,23,12,21,4,24,13,15], they often underutilize inherent ECG principles that provide strong inductive biases for physiologically consistent reconstruction. In this work, we emphasize the following two key claims grounded in such inherent properties:

Claim C1. Benefits of vector operations for limb lead reconstruction: If two limb leads are available, the remaining limb leads can be deterministically obtained via established vector operations (e.g., Einthoven's [7] and Goldberger's [8] equations) [11,6]. Therefore, rather than reconstructing all missing limb leads solely by learning-based translation, we advocate a *hybrid strategy*: we reconstruct only *one* additional limb lead using a learning model and then compute the remaining limb leads via vector operations, which reduces the learning burden while enforcing physiological consistency among limb leads. As shown in Fig. 1 left, the hybrid strategy consistently yields better performance than the learning-based strategy across representative baselines, supporting Claim C1.

Claim C2. Leveraging full limb leads for precordial lead reconstruction: Precordial leads represent cardiac activity on a plane that is geometrically distinct from limb leads. Hence, directly reconstructing six precordial leads from a single limb lead is intrinsically difficult. We argue that precordial lead reconstruction should be conducted *after* obtaining the full set of limb leads, since multiple limb leads provide richer information on coronal-plane activity and improve the fidelity of reconstructing precordial signals. Fig. 1 (right) shows that reconstruction RMSE improves as more limb leads are provided, supporting Claim C2 and motivating conditioning precordial reconstruction on full limb leads.

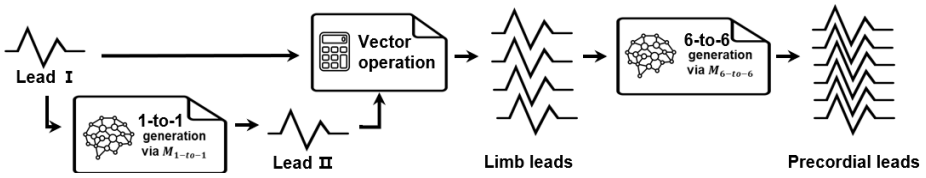

Fig. 2. The overview of AURORA. Here, $M_{1\text{-}to\text{-}1}$ and $M_{6\text{-}to\text{-}6}$ are our learning models IGUANA.

AURORA framework and IGUANA model. Based on C1 and C2, we propose a novel 12-lead ECG reconstruction framework, termed AURORA (**A**cc**U**rate Gene**R**ation **O**f the Standa**R**d 12-Le**A**d ECG), which judiciously combines learning models and physiological vector operations to reconstruct limb leads, followed by the reconstruction of precordial leads. To instantiate the learning components in AURORA, we further propose IGUANA (mult**I**-lead ECGs **G**eneration thro**U**gh le**A**d patter**N** le**A**rning), a lead-pattern learning model consisting of (i) a lead representation learner that converts cardiac feature information from the measured direction to the target lead direction and (ii) a lead generator that synthesizes the desired lead based on the transformed information.

Contributions. Our main contributions are summarized as follows: (1) We formulate two physiology-grounded claims for limb and precordial lead reconstruction and provide empirical evidence supporting them. (2) We propose AURORA, a hybrid framework that combines minimal learning with deterministic vector operations for accurate standard 12-lead ECG reconstruction from a single lead. (3) We propose IGUANA, a lead-pattern learning model integrated into AURORA, and demonstrate improved reconstruction quality and diagnostic utility through extensive experiments.

2 Our Framework: AURORA

In this section, we describe AURORA, our proposed framework based on our two claims C1 and C2.

Problem Definition. Let the i-th lead denoted by $L_i \in \mathbb{R}^n$, consisting of n samples. Each L_i corresponds to the i-th entry in the following order of 12-lead ECG: Leads I, II, III, aVR, aVL, aVF, and V1–V6, for $0 \leq i < 12$. The goal of reconstructing the standard 12-lead ECG from a single lead is to develop a framework f that accurately reconstructs the remaining eleven leads $L_{1:11} = \{L_1, L_2, \cdots, L_{11}\}$ from L_0 (Lead I). We formally formulate this problem as follows:

$$L_{1:11} = f(L_0).$$

Components of AURORA. Drawing from two key claims mentioned in Sections 1, we build our framework consisting of the following three primary steps (see Fig. 2):

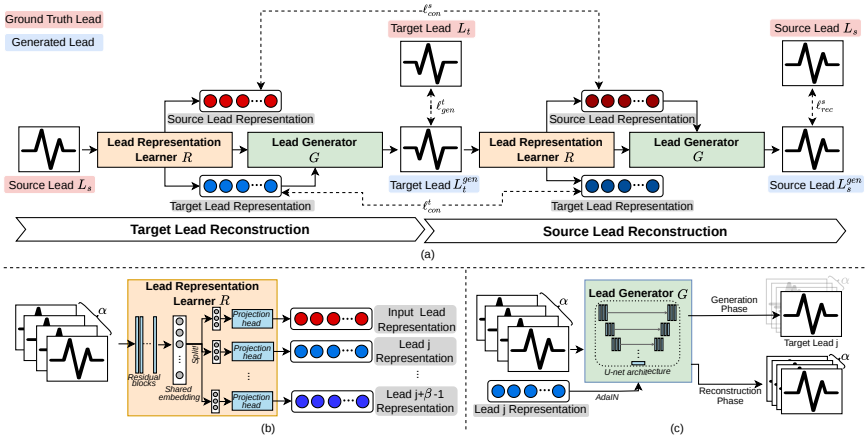

Fig. 3. Architecture of IGUANA. (a) illustrates the two-phase learning for the 1-to-1 instance . (b) and (c) depict the module-level implementation for the general $M_{\alpha\text{-}to\beta}$ setting: (b) the lead representation learner R, which builds a shared embedding and produces target-specific projections via multi-head projection heads, and (c) the lead generator G, implemented as a 1D U-Net conditioned via AdaIN to synthesize the corresponding target leads.

1. **reconstruction of Lead II from Lead I (referred to as 1-to-1 reconstruction)**: Using a single limb lead, Lead I, the 1-to-1 reconstruction aims to reconstruct an additional limb lead by using a learning-based model $M_{1\text{-}to\text{-}1}$. We use Lead II as the auxiliary limb lead throughout our experiments, as it was empirically found to be reliable for the 1-to-1 reconstruction stage and is physiologically informative, often aligning with the dominant cardiac electrical axis.
2. **reconstruction of remaining four limb leads**: From the two available limb leads (*i.e.*, Leads I and II) obtained from Step 1, we reconstruct the remaining four limb leads according to the following vector operations:

$$\text{Lead III} = \text{Lead II} - \text{Lead I}, \tag{1}$$
$$\text{Lead aVR} = -(\text{Lead I} + \text{Lead II})/2, \tag{2}$$
$$\text{Lead aVL} = (\text{Lead I} - \text{Lead III})/2, \tag{3}$$
$$\text{Lead aVF} = (\text{Lead II} + \text{Lead III})/2, \tag{4}$$

   where Eq. (1) is derived from Einthoven's triangle [7] and Eqs. (2)–(4) are from Goldberger's equations [8] (see Fig. 2 (b)).
3. **reconstruction of six precordial leads (referred to as 6-to-6 reconstruction)**: Using the six limb leads as input, the 6-to-6 reconstruction aims to reconstruct six precordial leads by using a deep-learning model $M_{6\text{-}to\text{-}6}$ (see Fig. 2 (c)).

Note that, as mentioned above, the AURORA framework encompasses two learning models, $M_{1\text{-}to\text{-}1}$ and $M_{6\text{-}to\text{-}6}$, which will be elaborated in the following section. Both $M_{1\text{-}to\text{-}1}$ and $M_{6\text{-}to\text{-}6}$ are instantiated by IGUANA (Fig. 3) with the same core architecture, but trained as separate instances with independent parameters.

3 Methodological Details: IGUANA

IGUANA defines a lead-to-lead translation *architecture* (a lead representation learner R and a lead generator G) and a unified training formulation. We use this design to build two *separate* models for AURORA: $M_{1\text{-}to\text{-}1}$ and $M_{6\text{-}to\text{-}6}$. These models share the same core architecture and objectives, but are *trained independently* with *separate parameters*. For clarity, we first describe the 1-to-1 model and then summarize the general $M_{\alpha\text{-}to\text{-}\beta}$ formulation, where the 6-to-6 model is obtained by setting $\alpha = \beta = 6$.

3.1 1-to-1 reconstruction in IGUANA

1-to-1 reconstruction Model We instantiate $M_{1\text{-}to\text{-}1}$ with IGUANA using two phases: *target reconstruction* and *source reconstruction*, where both phases share the same lead representation learner R and lead generator G. Given a source lead L_s (e.g., Lead I), the *target reconstruction* phase produces the target lead L_t (e.g., Lead II) as

$$L_t^{\text{gen}} = G\big(L_s,\, R(L_s, t)\big). \tag{5}$$

Then, the *source reconstruction* phase maps L_t^{gen} back to the source lead to encourage faithful transformation:

$$L_s^{\text{gen}} = G\big(L_t^{\text{gen}},\, R(L_t^{\text{gen}}, s)\big). \tag{6}$$

This shared two-phase training improves stability and encourages the generated lead to preserve source information. We reuse the same modules R and G in both the target and source reconstruction phases.

3.2 Optimization in IGUANA

Optimization We train $M_{1\text{-}to\text{-}1}$ with three loss functions: target reconstruction loss, source reconstruction loss, and representation-consistency loss (applied to both source and target representations).
Target reconstruction loss encourages accurate target synthesis:

$$\ell_{\text{gen}}^{t} = \text{RMSE}\big(L_t, L_t^{\text{gen}}\big). \tag{7}$$

Source reconstruction loss enforces source preservation via the reconstruction phase:

$$\ell_{\text{rec}}^{s} = \text{RMSE}\big(L_s, L_s^{\text{gen}}\big). \tag{8}$$

Representation-consistency loss aligns representations extracted from real and generated leads:

$$\ell^t_{\text{con}} = \left\| R(L_s, t) - R(L^{\text{gen}}_t, t) \right\|_1, \quad \ell^s_{\text{con}} = \left\| R(L^{\text{gen}}_t, s) - R(L_s, s) \right\|_1. \tag{9}$$

Finally, the overall objective is

$$\mathcal{L} = \lambda_{\text{gen}} ell^t_{\text{gen}} + \lambda_{\text{rec}}\, \ell^s_{\text{rec}} + \lambda_{\text{con}} \left(\ell^t_{\text{con}} + \ell^s_{\text{con}} \right), \tag{10}$$

where λ_{gen}, λ_{rec} and λ_{con} are weighting hyperparameters.

3.3 α-to-β reconstruction in IGUANA

IGUANA naturally extends to $M_{\alpha\text{-}to\text{-}\beta}$ by producing β target-specific projected representations from shared α source leads embedding. Conditioned on each target representation, the 1D U-Net [20] generator synthesizes the corresponding target lead via AdaIN-based [10] conditioning. We train this instance using the same two-phase (reconstruction/reconstruction) formulation and objectives described in Sections 3.1–3.2. In particular, $M_{6\text{-}to\text{-}6}$ is obtained by setting $\alpha = \beta = 6$ and training it as a separate instance with independent parameters. To maintain a unified I/O interface for G across the target reconstruction and source reconstruction phases, we fix the lead dimension of G to α. Accordingly, in the source reconstruction phase, G outputs α replicated candidates for each target lead and we select one as the final generated lead; in the reconstruction phase, G takes the α replicated generated leads as input to reconstruct the α source leads.

4 Experimental Evaluation

We conducted experiments to evaluate the effectiveness of our AURORA framework on two real-world 12-lead ECG datasets. Our evaluation focuses on: (i) overall reconstruction accuracy against state-of-the-art baselines, (ii) empirical validation of our two claims (C1/C2), and (iii) clinical utility via downstream disease prediction.

4.1 Experimental Settings

Datasets. We use two standard 12-lead ECG datasets from PhysioNet: PTB-XL [25] and CUSPH [26]. PTB-XL targets Myocardial Infarction and CUSPH targets Arrhythmia. They contain 21,799 and 45,152 recordings, respectively. Each recording is 10 seconds sampled at 500Hz (5,000 points) in the standard 12-lead setting.

Setting of AURORA. All ECG signals were sampled at 500 Hz and represented as 10-second segments with 5,000 samples. We used a patient-wise 7/1/2 split and lead-wise z-score normalization using training-set statistics. AURORA was trained with a batch size of 128 using 8 workers, and validation used a batch size of 16. The $M_{1-\text{to}-1}$ and $M_{6-\text{to}-6}$ stages were each trained for 300,000

Table 1. Overall reconstruction performance (average over 11 generated leads).

Dataset	Metric	Methods						
		Transformer	GAN	EKGAN	mEcgNet	ECGT2T	ANN128	AURORA
PTB-XL	RMSE ↓	0.198	0.184	0.163	0.158	0.153	0.146	**0.127**
	DTW ↓	9.787	8.564	7.879	7.774	7.510	7.072	**5.215**
	PCC ↑	0.162	0.340	0.505	0.531	0.594	0.665	**0.722**
CUSPH	RMSE ↓	1.020	0.934	0.805	0.778	0.733	0.705	**0.606**
	DTW ↓	21.578	19.570	16.080	15.540	14.201	13.527	**11.829**
	PCC ↑	0.202	0.363	0.472	0.488	0.530	0.609	**0.638**

iterations with an early stopping patience of 15. We used Adam with a learning rate of 1×10^{-5} and set all loss weights, i.e., λ_{gen}, λ_{rec}, and λ_{con}, to 1. For all baselines, we used the same split, preprocessing, input lead, and evaluation protocol; re-implemented baselines followed the original papers.

Competitors. We compare AURORA with Transformer [23], ECG-GAN [14], EKGAN [13], mEcgNet [15], ECGT2T [12], and ANN128 [21]. Since the official implementations of ECG-GAN, mEcgNet, and ECGT2T are not publicly available, we implemented them following the original papers and obtained comparable performance to the reported results.

Evaluation Metrics. We report RMSE [16], DTW [18], and PCC [5]. Lower RMSE/DTW and higher PCC indicate better reconstruction performance.

4.2 Results and Analyses

Overall Reconstruction Accuracy. Table 1 summarizes the average reconstruction performance over the 11 reconstructed leads on PTB-XL and CUSPH. AURORA achieves the best performance across all metrics on both datasets. On PTB-XL, AURORA reduces RMSE from 0.146 (ANN128) to 0.127 (13.0%) and DTW from 7.072 to 5.215 (26.3%), while improving PCC from 0.665 to 0.722 (+0.057). On CUSPH, AURORA reduces RMSE from 0.705 (ANN128) to 0.606 (14.0%) and DTW from 13.527 to 11.829 (12.6%), and increases PCC from 0.609 to 0.638 (+0.029). We also observed consistent gains over baselines on each limb and precordial leads (not shown due to space).

Clinical Utility via Disease Prediction. We further evaluate whether the reconstructed 12-lead ECG preserves disease-relevant information by performing downstream disease prediction. Following prior work, we adopt ResNet18 [9] with a 1D convolutional architecture as the prediction model and use AUROC and AUPRC as evaluation metrics. As shown in Fig. 4, AURORA achieves diagnostic performance very close to that obtained using the original 12-lead ECG. In particular, for myocardial infarction (PTB-XL), the decrease from the original ECG is only 0.63% (AUROC) and 0.11% (AUPRC), and for arrhythmia (CUSPH), the decrease is 0.71% (AUROC) and 1.55% (AUPRC). These results suggest

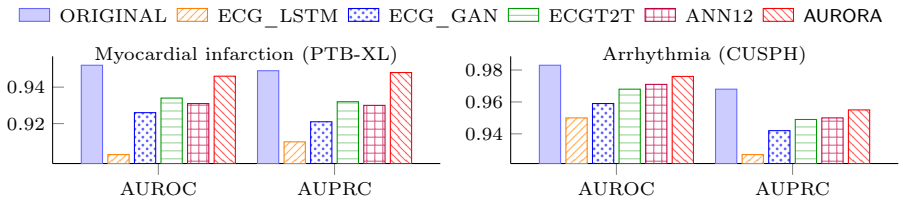

Fig. 4. Prediction accuracy of two types of cardiovascular diseases in terms of AUROC and AUPRC (the higher the better). The standard 12-lead ECG corresponds to either the original leads measured in hospitals or the ones generated by three competitors and AURORA from Lead I.

Table 2. Ablation results. (a) validates hybrid strategy and two-stage reconstruction. (b) shows the effect of removing losses.

	RMSE	DTW	PCC
AURORA$_{1to11}$	0.133	5.462	0.707
AURORA$_{noVec}$	0.131	5.322	0.708
AURORA	**0.127**	**5.215**	**0.722**

(a)

	RMSE	DTW	PCC
AURORA$_{w/o\ RL}$	0.144	5.805	0.660
AURORA$_{w/o\ RCL}$	0.143	5.689	0.670
AURORA	**0.127**	**5.215**	**0.722**

(b)

that AURORA effectively preserves clinically meaningful characteristics, thereby mimicking the diagnostic capacity of hospital-acquired 12-lead ECG using only a single lead as input.

Validation of Claims C1 and C2. To validate the efficacy of our two claims—(C1) the hybrid strategy for limb lead reconstruction and (C2) the two-stage strategy that reconstructs limb leads first and precordial leads thereafter—we compare AURORA with two variants: (i) AURORA$_{1to11}$, which reconstructs all remaining leads at once from Lead I using only the learning model; and (ii) AURORA$_{noVec}$, which reconstructs limb leads without vector operations and then reconstructs precordial leads conditioned on the reconstructed limb leads. Table 2 (a) reports the results. AURORA consistently outperforms both variants across all metrics, demonstrating the benefit of explicitly incorporating vector operations for limb leads and adopting the two-stage reconstruction pipeline.

Effectiveness of Our Loss Function. We conduct a compact ablation study to assess whether the proposed loss terms are beneficial for training IGUANA. We compare the full model with two variants: AURORA$_{\text{w/o } RL}$ removes the source reconstruction loss and uses only the target reconstruction and representation-consistency losses, and AURORA$_{\text{w/o } RCL}$ removes the representation-consistency loss and uses only the target and source reconstruction losses. Table 2 (b) shows that removing either loss term consistently degrades reconstruction performance across metrics, highlighting the importance of both reconstruction and representation consistency in accurate lead-to-lead reconstruction.

5 Conclusions

We addressed standard 12-lead ECG reconstruction from a single measured lead by leveraging inherent ECG principles. We validated two claims: deterministic vector operations improve limb-lead reconstruction, and conditioning precordial-lead reconstruction on the full set of limb leads improves fidelity. Based on these claims, we proposed **AURORA**, a three-step framework (1-to-1 reconstruction, vector operations for limb leads, and 6-to-6 reconstruction for precordial leads) instantiated with **IGUANA**. Experiments on PTB-XL and CUSPH show that AURORA outperforms competitive baselines in reconstruction metrics and preserves clinically meaningful information in downstream disease prediction close to the original 12-lead ECG.

Acknowledgements. This is the result of the collaboration between Hanyang University and Medical AI Inc. The work of Sang-Wook Kim was supported by Institute of Information & Communications Technology Planning & Evaluation (IITP) grants funded by the Korea government (MSIT) (No. RS-2022-00155586, A High-Performance Big-Hypergraph Mining Platform for Real-World Downstream Tasks; No. IITP-2026-RS-2026-25544375, Leading Generative AI Human Resources Development; and No. RS-2020-II201373, Artificial Intelligence Graduate School Program (Hanyang University)). The work of Won-Yong Shin was supported by the National Research Foundation of Korea (NRF) grant funded by the Korea government (MSIT) (No. RS-2021-NR059723).

Disclosure of Interests. Yong-Yeon Jo and Junmyung Kwon are affiliated with Medical AI Inc. The remaining authors declare no competing interests relevant to the content of this article.

References

1. Alnasser, S., Alkalthem, D., Alenazi, S., Alsowinea, M., Alanazi, N., Al Fagih, A., Alnasser, S.K., Alanzai, N.: The reliability of the apple watch's electrocardiogram. Cureus **15**(12) (2023)
2. Azram, M., Ahmed, N., Leese, L., Brigham, M., Bowes, R., Wheatcroft, S.B., Ngantcha, M., Stegemann, B., Crowther, G., Tayebjee, M.H.: Clinical validation and evaluation of a novel six-lead handheld electrocardiogram recorder compared to the 12-lead electrocardiogram in unselected cardiology patients (evalecg cardio). European Heart Journal-Digital Health **2**(4), 643–648 (2021)
3. Bouzid, Z., Al-Zaiti, S.S., Bond, R., Sejdić, E.: Remote and wearable ecg devices with diagnostic abilities in adults: a state-of-the-science scoping review. Heart Rhythm **19**(7), 1192–1201 (2022)
4. Brophy, E.: Synthesis of dependent multichannel ecg using generative adversarial networks. In: Proceedings of the 29th ACM international conference on information & knowledge management. pp. 3229–3232 (2020)

5. Cohen, I., Huang, Y., Chen, J., Benesty, J., Benesty, J., Chen, J., Huang, Y., Cohen, I.: Pearson correlation coefficient. Noise reduction in speech processing pp. 1–4 (2009)
6. De Luna, A.B.: Clinical electrocardiography: a textbook. John Wiley & Sons (2012)
7. Einthoven, W., Fahr, G., DEWAART, A.: Ueber die richtung und die manifeste grssse der potentialschwankungen in menschlichen herzen under fiber den einfluss der herzlage aufdie form des elecktrokardiogramms. Arch des Physiol **150**, 275 (1913)
8. Goldberger, E.: The avl, avr, and avf leads: a simplification of standard lead electrocardiography. American Heart Journal **24**(3), 378–396 (1942)
9. He, K., Zhang, X., Ren, S., Sun, J.: Deep residual learning for image recognition. In: Proceedings of the IEEE conference on computer vision and pattern recognition. pp. 770–778 (2016)
10. Huang, X., Belongie, S.: Arbitrary style transfer in real-time with adaptive instance normalization. In: Proceedings of the IEEE international conference on computer vision. pp. 1501–1510 (2017)
11. James, W.B., Williams, H.B.: The electrocardiogram in clinical medicine. The American Journal of the Medical Sciences (1827-1924) **140**(5), 644 (1910)
12. Jo, Y.Y., Choi, Y.S., Jang, J.H., Kwon, J.M.: Ecgt2t: Towards synthesizing twelve-lead electrocardiograms from two asynchronous leads. In: ICASSP 2023-2023 IEEE International Conference on Acoustics, Speech and Signal Processing (ICASSP). pp. 1–5. IEEE (2023)
13. Joo, J., Joo, G., Kim, Y., Jin, M.N., Park, J., Im, H.: Twelve-lead ecg reconstruction from single-lead signals using generative adversarial networks. In: International Conference on Medical Image Computing and Computer-Assisted Intervention. pp. 184–194. Springer (2023)
14. Lee, J., Oh, K., Kim, B., Yoo, S.K.: Synthesis of electrocardiogram v-lead signals from limb-lead measurement using r-peak aligned generative adversarial network. IEEE journal of biomedical and health informatics **24**(5), 1265–1275 (2019)
15. Lee, J., Yoo, Y., Kim, J., Lim, D., Yang, G., Yoo, C.: Parameter-efficient 12-lead ecg reconstruction from a single lead. In: International Conference on Medical Image Computing and Computer-Assisted Intervention. pp. 431–441. Springer (2025)
16. Legendre, A.M.: Nouvelles méthodes pour la détermination des orbites des comètes: avec un supplément contenant divers perfectionnemens de ces méthodes et leur application aux deux comètes de 1805. Courcier (1806)
17. Li, K., Elgalad, A., Cardoso, C., Perin, E.C.: Using the apple watch to record multiple-lead electrocardiograms in detecting myocardial infarction: where are we now? Texas Heart Institute Journal **49**(4), e227845 (2022)
18. Müller, M.: Dynamic time warping. Information retrieval for music and motion pp. 69–84 (2007)
19. Pinto, J.R., Cardoso, J.S., Lourenço, A.: Evolution, current challenges, and future possibilities in ecg biometrics. IEEE Access **6**, 34746–34776 (2018)
20. Ronneberger, O., Fischer, P., Brox, T.: U-net: Convolutional networks for biomedical image segmentation. In: International Conference on Medical image computing and computer-assisted intervention. pp. 234–241. Springer (2015)
21. Savostin, A., Koshekov, K., Ritter, Y., Savostina, G., Ritter, D.: 12-lead ecg reconstruction based on data from the first limb lead. Cardiovascular Engineering and Technology **15**(3), 346–358 (2024)
22. Singh, M., Rao, R., Gupta, S.: Kardiamobile for ecg monitoring and arrhythmia diagnosis. American family physician **102**(9), 563–564 (2020)

23. Sohn, J., Yang, S., Lee, J., Ku, Y., Kim, H.C.: Reconstruction of 12-lead electrocardiogram from a three-lead patch-type device using a lstm network. Sensors **20**(11), 3278 (2020)
24. Ukil, A., Marin, L., Jara, A.J., Farserotu, J.: Human-centric analytics and systems impacting quality of life: Ecg analytics and beyond. In: Proceedings of the 30th ACM International Conference on Information & Knowledge Management. pp. 4884–4885 (2021)
25. Wagner, P., Strodthoff, N., Bousseljot, R.D., Kreiseler, D., Lunze, F.I., Samek, W., Schaeffter, T.: Ptb-xl, a large publicly available electrocardiography dataset. Scientific data **7**(1), 154 (2020)
26. Zheng, J., Zhang, J., Danioko, S., Yao, H., Guo, H., Rakovski, C.: A 12-lead electrocardiogram database for arrhythmia research covering more than 10,000 patients. Scientific data **7**(1), 48 (2020)